
RUNOUT ANALYSIS USING THE MATERIAL POINT METHOD (MPM) FOR CDA CASES 2A AND 2B

AUTHORS

Erick Lino Ramírez, MSc., SRK Consulting (Canada) Inc., Vancouver, BC, Canada
Osvaldo Ledesma, Ph.D., SRK Consulting (Canada) Inc., Vancouver, BC, Canada
Arcesio Lizcano, Ph.D., SRK Consulting (Canada) Inc., Vancouver, BC, Canada

ABSTRACT

Traditional dam-break flood models were developed to predict flooding caused by water reservoir failures, using approaches such as physical erosion models, weir-based formulations, empirical breach equations, and comparative case analysis (USBR 1988). Although not originally developed for tailings dams, these methods are still widely used, often with limited adaptation, in tailings dam breach analysis (TDBA), now required under the global mining standard (ICMM 2020) following several catastrophic failures.

In 2021, the Canadian Dam Association (CDA) published a Technical Bulletin on Tailings Dam Breach Analysis (CDA 2021) to provide guidance for estimating the consequences of tailings dam failures. Prior to its release, limited guidance existed for conducting such analyses. The bulletin defines four representative TDBA cases based on the presence of supernatant water and the liquefaction potential of the tailings. These are grouped into two post-failure flow regimes: water-laden tailings flows (Cases 1A and 1B), characterized by hydraulic entrainment, and solids-dominated releases (Cases 2A and 2B), governed primarily by the mechanical failure of tailings.

While software tools such as HEC-RAS, FLOW-3D, or MADFLOW are mentioned in CDA (2021) as commonly used for TDBA, this paper proposes the Material Point Method (MPM), a numerical method suited for large-deformation problems, as an alternative for estimating runout distances in solids-dominated scenarios. MPM is based on continuum mechanics and is gaining attention in the geotechnical community for its ability to simulate post-failure behavior. Methodology is illustrated through three applications, including the runout assessment of a waste rock dump facility.

RÉSUMÉ

Les modèles traditionnels d'inondation par rupture de barrage ont été conçus pour prédire les crues résultant de la défaillance de réservoirs d'eau, à l'aide de modèles physiques d'érosion, de formulations basées sur les déversoirs, d'équations empiriques de brèche et d'analyses comparatives de cas (USBR 1988). Bien que ces méthodes n'aient pas été initialement développées pour les barrages de résidus, elles restent largement utilisées, souvent avec des adaptations limitées, dans l'analyse de la rupture des barrages de résidus (TDBA), aujourd'hui exigée par la norme minière mondiale (ICMM 2020) après plusieurs accidents catastrophiques.

En 2021, l'Association canadienne des barrages (ACB) a publié un article technique sur la TDBA afin de fournir des recommandations pour l'estimation des conséquences de rupture. Avant cela, les orientations pour de telles analyses étaient très limitées. Cet article identifie quatre cas représentatifs de TDBA selon la présence d'eau surnageante et le potentiel de liquéfaction des résidus, regroupés en deux régimes post-rupture : les flots de résidus chargés en eau (cas 1A/1B, avec entraînement hydraulique) et les relâchements dominés par les solides (cas 2A/2B, sous contrôle mécanique).

Bien que des logiciels comme HEC-RAS, FLOW-3D ou MADFLOW soient couramment employés (ACB 2021), cet article propose la méthode des points matériels (MPM), adaptée aux grandes déformations, comme alternative pour estimer les distances de déplacement dans les scénarios dominés par les solides. La MPM, basée sur la mécanique des milieux continus, gagne en importance pour simuler le comportement après rupture. Trois exemples d'application, dont l'étude d'un dépôt de stériles, illustrent la méthodologie.

1 INTRODUCTION

Traditional dam-breach analyses were developed to predict inundation zones resulting from failures of water-retaining dams. These methods focus on defining the breach hydrograph and its peak discharge, which is then routed downstream. Methodologies are categorized into four types: (1) physically-based models, which predict breach development and outflow using an erosion model; (2) parametric models, which estimate breach behavior using dam characteristics (e.g., height, volume) and weir equations; (3) predictor equations, which derive peak discharge estimates from historical data; and (4) comparative analysis, which applies to dams with characteristics similar to a failed structure (USBR 1998).

Tailings dam failures present different challenges. Unlike water, tailings are non-Newtonian materials with diverse flow behaviors, ranging from water-like flows (e.g., water flood, mud flood, mudflow) to friction-dominated runouts (e.g., flow slide, slumping failure) (Williams et al., 2023). Failures often involve partial mobilization of tailings through mechanisms such as collapse, overtopping, or seepage. Recent failures, including the 2008 Xiangfen collapse in China (Wei et al. 2013), the 2014 Mount Polley failure in Canada (Morgenstern et al. 2015), the 2015 Fundão catastrophe in Brazil (Morgenstern et al. 2016), and the 2019 Brumadinho disaster in Brazil (Robertson et al. 2019), have highlighted the need for improved dam safety practices. In response, the mining industry developed the Global Industry Standard on Tailings Management (ICMM 2020) with the objective of achieving zero harm to people and the environment. A requirement of this standard is conducting Tailings Dam Breach Analyses (TDBA) to identify risks to public safety and the environment, leading to increased demand for approaches tailored to tailings behavior.

In 2021, the Canadian Dam Association (CDA) released the Technical Bulletin for TDBA to standardize methodologies for assessing tailings dam breaches. The bulletin incorporates findings from previous workshops (Chen et al. 2014; Martin et al. 2015; Small et al. 2017) and emphasizes the importance of hydrodynamic and geomechanical modeling of tailings flows. The bulletin identifies two critical factors in breach analysis: the presence of supernatant pond and the liquefaction potential of tailings (Martin et al. 2019). Based on these factors, four TDBA cases are defined. Cases 1A and 1B involve supernatant ponds, with liquefiable tailings in Case 1A but not in Case 1B. Cases 2A and 2B lack supernatant ponds and differ in tailings liquefaction potential. These cases correspond to two physical processes: Process I, involving water discharge transporting tailings and dam materials (Cases 1A, 1B), and Process II, involving the release of tailings solids without significant fluid discharge (Cases 2A, 2B).

For Cases 2A and 2B, the CDA (2021) recommends hydrodynamic modeling tools with non-Newtonian capabilities or geomechanical modeling tools based on mass and momentum equations to simulate the runout. While tools such as HEC-RAS, FLOW-3D or MADFLOW are referenced, this paper proposes the Material Point Method (MPM) as an alternative for assessing runout distances in Cases 2A and 2B. MPM is a continuum-based, particle method, capable of handling large deformations without the mesh distortion issues of traditional methods like the Finite Element Method (FEM). Although MPM has potential for modeling tailings dam failures, its application in engineering practice remains limited.

To demonstrate the suitability of MPM for Cases 2A and 2B, this paper presents the methodology used to estimate runout distances, followed by three application examples. These examples aim to show the MPM capabilities in handling complex runout processes under various scenarios.

2 MATERIAL POINT METHOD

The Material Point Method (MPM) was developed to capture large deformations in history-dependent materials (Sulsky et al. 1994, 1995). It was presented as an extension of the particle-in-cell (PIC) method originally used to model fluid flow. In MPM, the continuum is represented by Lagrangian points (material points or particles) that move through a fixed Eulerian mesh. These particles carry the physical properties of the continuum: mass, momentum, material parameters, velocities, strains, stresses, external loads, and state variables of the constitutive model. The mesh carries no permanent information.

At the beginning of each time step, the particles transfer their information to the mesh nodes. Figure 1a shows the particles and nodes as red circles (p) and empty squares (i), respectively. The equation of motion is solved at the nodes to obtain accelerations, which are integrated to compute nodal velocities. These velocities are shown as blue arrows in Figure 1b. The computed nodal values are then mapped back to the particles to update stresses, strains, and positions (Figure 1c). At the end of the time step, since the mesh carries no permanent information, it is reset to the initial configuration (Figure 1d). This approach combines the advantage of Eulerian and Lagrangian formulations. A fixed background mesh (Eulerian) prevents mesh distortion, while moving material points (Lagrangian) carry the history of physical properties, enabling accurate simulation of large deformation. For mathematical formulation details see Al-Kafaji (2013), Ceccato (2015), Yerro (2015), and Fern et al. (2019).

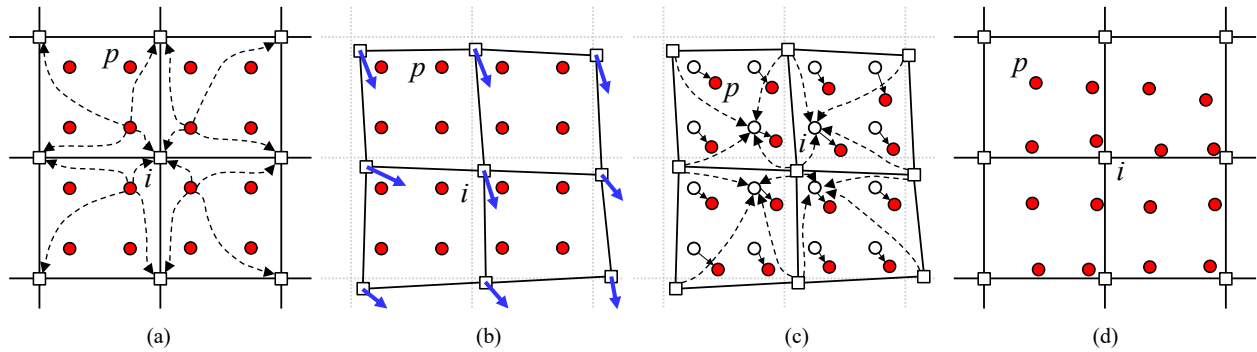


Figure 1: MPM algorithm procedure (Lino Ramírez E. 2021)

In recent years, MPM has been applied in geotechnical problems, including runout analyses of slopes and landslides (Yerro et al. 2016; Yerro et al. 2019), static liquefaction in slopes and tailings dams (Cuomo et al. 2019; Lino Ramírez E. 2021), and simulations of tailings dam failures such as the Feijão failure (Robertson et al. 2019) and the Cadia TSF failure (Macedo et al. 2024). These studies confirm MPM's suitability for TDBA in CDA Cases 2A and 2B, where solid-to-solid and solid-to-fluid interactions dominate due to the absence of supernatant water, which otherwise leads to fluid-to-fluid interactions in Cases 1A and 1B. For these cases, the one-phase single-point MPM formulation is appropriate, as used in the simulations presented in this work.

More advanced multi-phase formulations, such as the two-phase double-point MPM, are better suited for CDA Cases 1A and 1B, which involve supernatant water (Ceccato et al. 2021; Yerro et al. 2022). However, these formulations are still under development and have limited use in engineering practice, but may see wider use in the future.

All simulations in this paper were performed with Anura3D (2024), a software used in recent geomechanics studies (Alonso, 2021; Lino Ramírez et al. 2023; Di Carluccio et al. 2024).

3 METHODOLOGY

The methodology used in this study employs the one-phase single-point MPM formulation to estimate the runout distance of CDA Cases 2A and 2B. The process involves identifying the failure modes to be analyzed, constructing the boundary value problem, and initiating movement through the strength reduction of a predefined low-strength zone.

The first step is to identify the failure modes under consideration. For Case 2A, failure occurs as a flow-type slope instability caused by the liquefaction of loose, saturated contractive tailings. For Case 2B, it involves a slumping-type slope failure associated with non-liquefiable tailings. Once the failure modes are defined, the boundary value problem is constructed using a 2D or 3D MPM framework, depending on the complexity of the geometry and the objectives of the analysis.

A low-strength zone is incorporated into the model and assigned initial properties that allow the system to reach equilibrium under static loading. After equilibrium is achieved, the shear strength of the low-strength zone is reduced abruptly to trigger instability and initiate runout. This simplification is considered reasonable, as the focus of the simulation is on the post-failure behavior (e.g., the mobilization and runout of tailings) rather than accurately representing the mechanisms that lead to the onset of failure. The low-strength zone conceptually represents conditions such as a pre-existing weak layer or the buildup of excess pore water pressure due to monotonic or cyclic loading that may lead to static or seismic liquefaction.

The simulation process follows these steps:

1. Definition of geometry and geotechnical units, specifying the constitutive model and relevant physical and mechanical parameters for each material.
2. Definition of the initial number of material points per element, which ensures sufficient resolution for accurate simulations.
3. Definition of boundary conditions, such as fixed or roller boundaries to replicate the physical constraints on the model.
4. Meshing of the geometry, creating the background grid needed for the MPM framework as described in Section 2.
5. Solving the boundary value problem to achieve static equilibrium, using the initially defined material properties to balance all forces in the system.
6. Initiating the dynamic phase of the simulation (movement) by abruptly reducing the shear strength of the low-strength zone to set off failure and compute the resulting runout.

4 APPLICATION EXAMPLES

This section presents three application examples of runout analysis using MPM for CDA Cases 2A and 2B. These examples illustrate different failure scenarios and demonstrate the applicability of the methodology presented in Section 3. For each example, the objective is to estimate the runout distance following the onset of failure, based on the characteristics of the identified low-strength zones. None of these examples is a back-analysis of an actual failure, although each is based on real facilities.

Table 1 summarizes the key details of each case: facility type, project phase, CDA classification, characteristics of the low-strength zone, and objective of the analysis.

Table 1: Application Examples

ID	Description	Project Phase	CDA Case	Low-strength zone characteristics	Objective
Example 1	Upstream tailings dam	Not operational	Case 2A	Mobilization of red mud tailings remolded strength.	Estimate runout distance
Example 2	Filtered tailings dam	Design	Case 2B	Saturated, contractive tailings at the base of the dam	Estimate runout distance
Example 3	In-pit waste rock dump	Design	Case 2B	Pre-existing weak layer	Assess berm containment

4.1 Example 1: Upstream Tailings Dam (Case 2A)

The first case examines the potential failure of an upstream tailings dam located in Germany, which is currently not in operation. Figure 2 shows the geometry and the materials. The dam is located within a shallow excavation, reaching depths of up to approximately 3 m, in underlying Quaternary gravel deposits. Containment is achieved through a series of upstream embankment raises, constructed using a combination of locally sourced borrow material and compacted bauxite residues.

The outer embankment has a single bench midway up the overall slope with approximately 12m height above the surrounding ground. The overall slope angle is about 30 degrees, while the inter-bench slope angle is close to 35 degrees (approximately 1.4H:1V). The single bench that divides the slope has a minimum width of about 4m. This tailings dam does not have a supernatant pond in current conditions, and the soft red mud material was identified as susceptible to liquefaction. Therefore, it is classified as Case 2A according to CDA (2021).

The potential failure mode evaluated in the dam breach analysis was described as: “a regional seismic event triggers the mobilization of the remolded shear strength of soft red mud tailings. This leads to a rotational failure and releases tailings into the environment.”

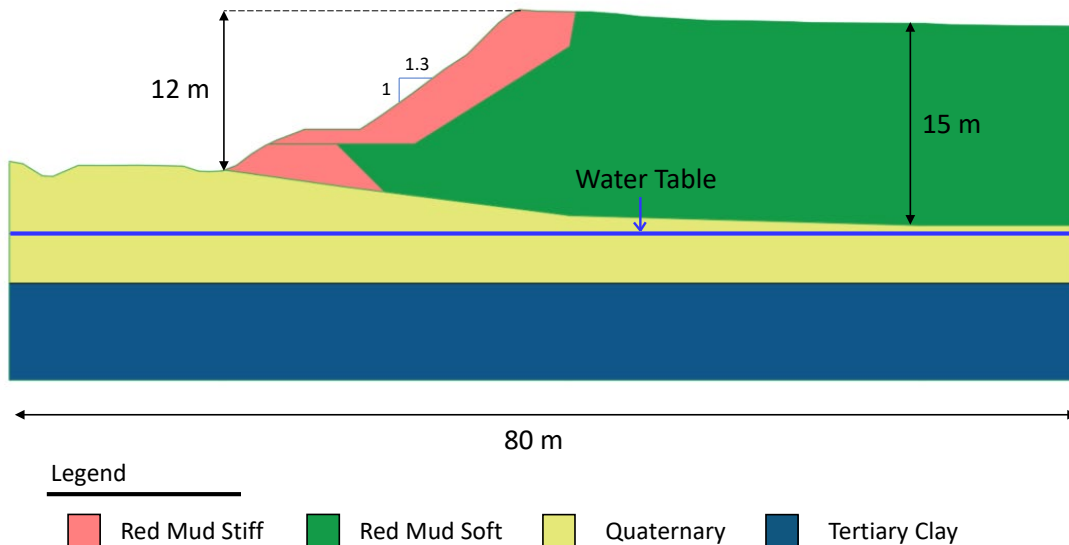


Figure 2: Example 1 – Upstream Tailings Dam

The MPM model is shown in Figure 3 highlighting the initial distribution of material points and background mesh. The simulation used three material points per element. The mesh was refined in critical areas and extended beyond the initial configuration of the tailings dam, as the MPM framework require empty

elements to accommodate material points that move during the deformation process. In total, the model included 38,004 material points and 19,305 triangular elements. The Mohr-Coulomb model was used for all materials, with material parameters (summarized in Table 2) determined based on field investigation data and engineering judgment.

Table 2: Material parameters to achieve equilibrium – Example 1

Parameter	Symbol	Unit	Red Mud Soft	Red Mud Stiff	Quaternary	Tertiary Clay
Unit weight	γ	kN/m ³	18	18	18	18
Young Modulus	E	MPa	10	40	40	20
Poisson ratio	ν	[-]	0.2	0.2	0.2	0.2
Friction angle	ϕ	°	30	30	35	17
Cohesion	c	kPa	0	5	0	10

The soft red mud tailings were classified as high to medium plasticity clay, with a clay content of 43%, a plasticity index of 23.6%, a liquid limit of 49.5%, a water content of 39% and a specific gravity of 3.0. This material (highlighted in blue in Figure 3) was identified as susceptible to a sudden loss of shear strength due to its thixotropic behavior, mobilizing its remolded shear strength. The remolded shear strength (s_u) was estimated using the liquidity index, as suggested by Leroueil, 1983.

Following the methodology outlined in Section 3, the runout analysis was performed using the 2D MPM model prepared for the geometry shown in Figure 2. For this example, the low-strength layer was assigned to the soft red mud material (blue area in Figure 3), representing the zone prone to instability. Two runout scenarios were analyzed by abruptly reducing the initial shear strength of the red mud layer. The initial strength was defined by $\phi = 30^\circ$ and $c = 0$ kPa, and was reduced to $c = s_u = 5$ kPa and 2 kPa, with $\phi = 0^\circ$ for both cases, based on the available data.

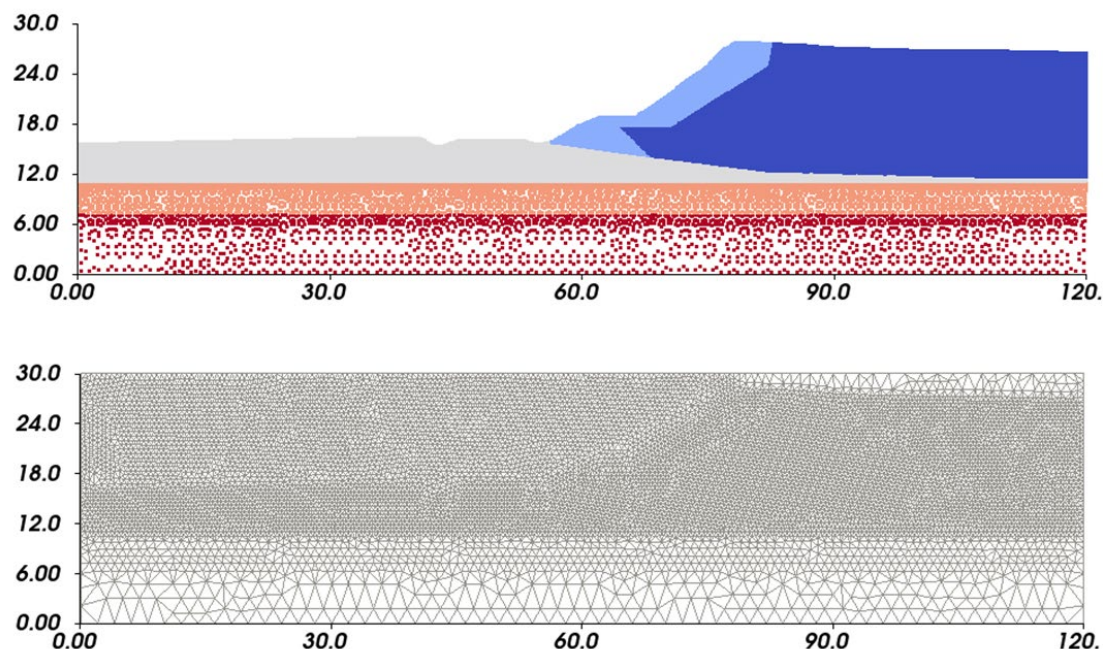


Figure 3: Example 1 – MPM model

The simulation results are shown in Figures 4 and 5, illustrating the progression of the deformed shape and deviatoric strains over time. Figure 4 presents the results for a remolded shear strength of 5 kPa, while Figure 5 shows the results for a shear strength of 2 kPa in the soft red mud.

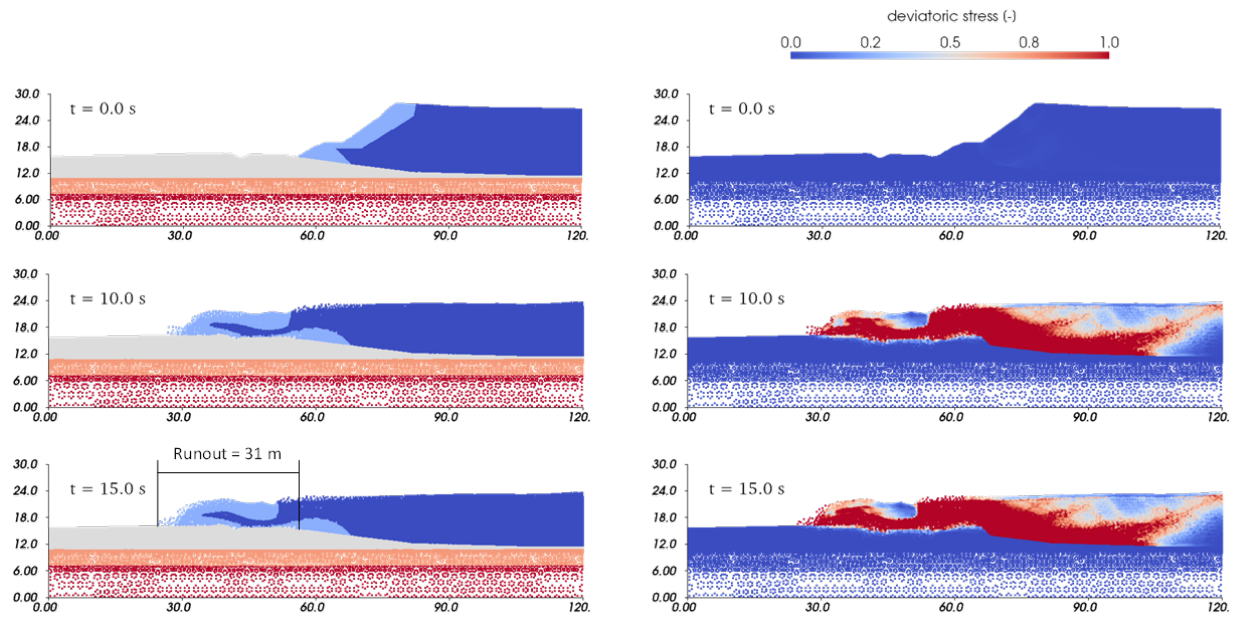


Figure 4: Example 1 – Runout Assessment ($s_u = 5$ kPa)

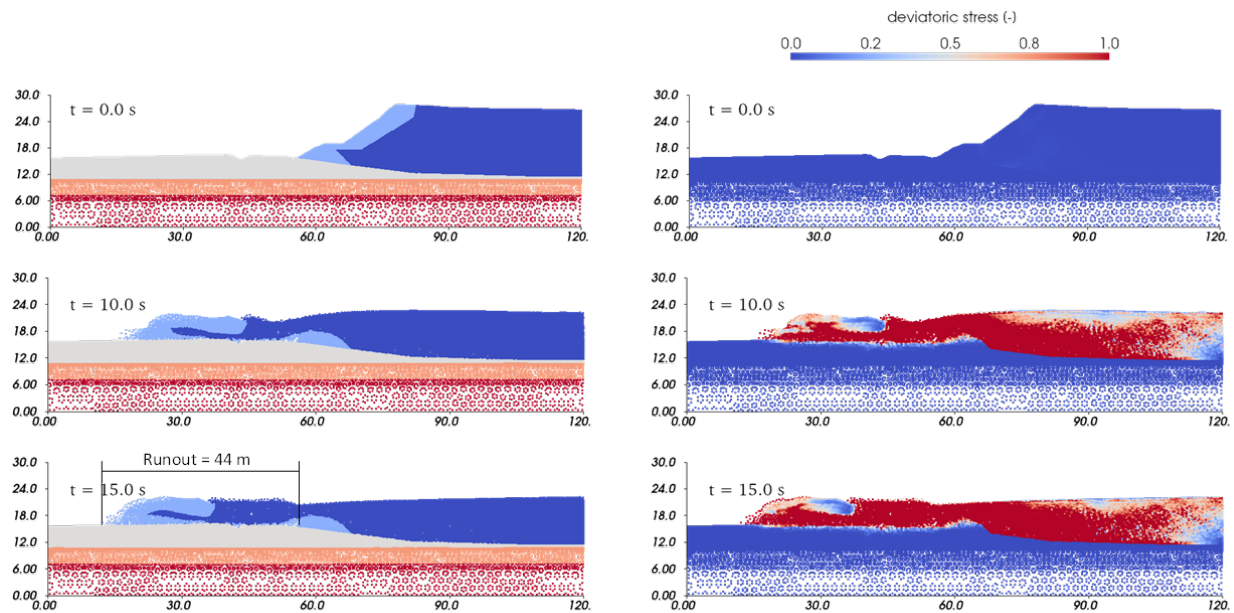


Figure 5: Example 1 – Runout Assessment ($s_u = 2$ kPa)

In both analyzed scenarios, the runout distance is defined as the horizontal distance between the initial toe position of the embankment and its final toe position after reaching equilibrium. This distance is distinct from the maximum displacement experienced by any individual material point within the embankment. For the base case scenario ($s_u = 5$ kPa), the estimated runout distance is 31 m. For the scenario with $s_u = 2$ kPa, the runout distance is 44 m.

4.2 Example 2: Filtered Tailings Dam (Case 2B)

The second example analyzes the potential failure of a filtered tailings dam located in Mexico, currently in the design phase. Figure 6 illustrates the geometry and materials. The planned structure consists of compacted sand-like tailings placed in 30 cm thick horizontal layers. A liner is installed at the base to prevent contact water from seeping into the foundation aquifer. The total dam height is 57 m, including a 6.6 m starter dam with 2.5H:1V slopes. The overall slope angle is approximately 19 degrees; the inter-bench slope angle is around 22 degrees (2.5H:1V). The dam lacks a supernatant pond, and the compacted filtered tailings are not susceptible to liquefaction. Therefore, it is classified as Case 2B according to CDA (2021).

The potential failure mode considered in the analysis was defined as: “the failure of the liner at the base of the filtered tailings dam allows water from the subdrainage system to infiltrate, leading to the saturation of the lower 2 meters of filtered tailings. As construction advances, this saturated layer experiences a significant reduction in shear strength, triggering a global failure and releasing filtered tailings into the environment.”

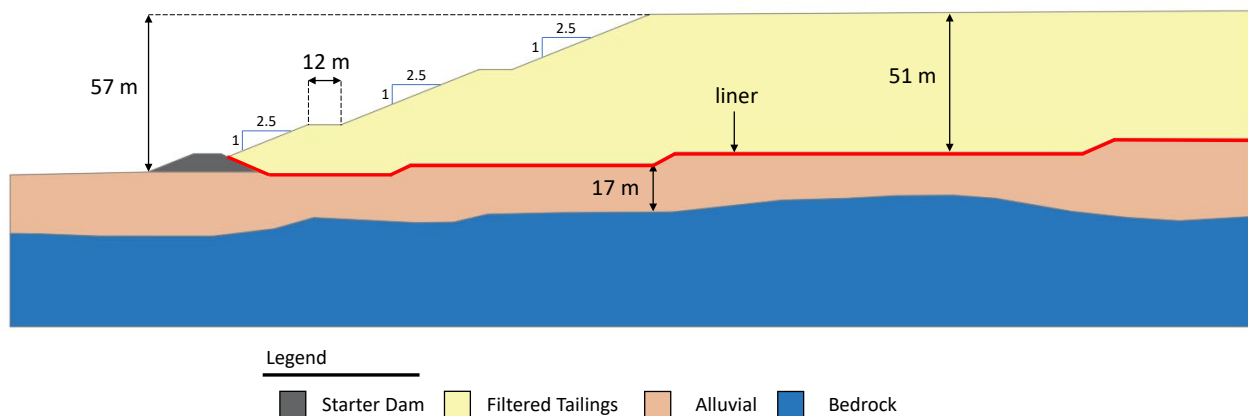


Figure 6: Example 2 – Filtered Tailings Dam

Figure 7 shows the initial distribution of material points in the MPM model. The 2D simulation used three material points per element, totaling 21,514 material points and 10,204 triangular elements. As in Example 1, the Mohr-Coulomb model was used. The filtered tailings from the plant site exhibit moisture content between 13 and 20% and a specific gravity of 3, yielding a volumetric solids content ranging of 63 –72%. According to CDA (2021), this range supports classification as Case 2B, where a slumping -type behavior is anticipated (O’Brien, 1986). Table 3 lists the material parameters used.

Table 3: Material parameters to achieve equilibrium – Example 2

Parameter	Symbol	Unit	Filtered Tailings	Started Dam	Liner	Alluvial	Rock
Unit weight	γ	kN/m ³	18	18	18	18	20
Young Modulus	E	MPa	15	40	10	10	80
Poisson ratio	ν	[-]	0.2	0.2	0.2	0.2	0.2
Friction angle	ϕ	°	33	35	21	34	44
Cohesion	c	kPa	0	0	0	10	100

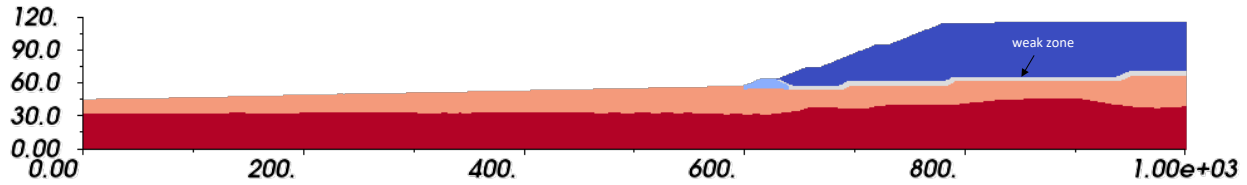


Figure 7: Example 2 – MPM model

As in Example 1, the methodology described in Section 3 was followed. The runout analysis used a 2D MPM model corresponding to the geometry in Figure 6. The low-strength zone was defined as the lower 2 m of filtered tailings, assumed to become saturated due to liner failure. The system was first brought to static equilibrium. Then, movement was initiated by abruptly reducing the shear strength of the low-strength zone from $\phi = 33^\circ$ and $c = 0$ kPa to $\phi = 0^\circ$ and $c = s_u = 5$ kPa.

Figure 8 illustrates the deformed shape and deviatoric strains over time. The results show that under the assumed failure mode, the dam may overtop, releasing filtered tailings into the environment. The estimated runout distance is approximately 18 m.

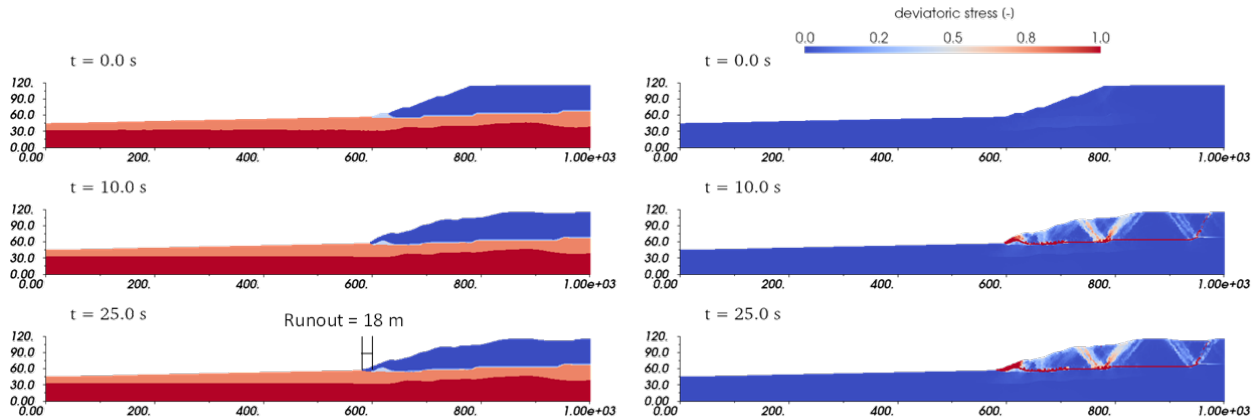


Figure 8: Example 2 – Runout Assessment

4.3 Example 3: In-Pit Waste Rock Dump Failure (Case 2B)

The third example assesses the potential runout of an in-pit waste rock dump in Peru, currently in the design phase. Figure 9 shows the geometry and materials. The planned dump is 400 m height and includes an 80 m wide safety berm separating it from the nearest open pit. The overall slope angle is approximately 23 degrees (2.4H:1V). Inter-benches are 43.5 m wide and 40 m high, with an inter-bench slope angle of 37 degrees (1.33H:1V). Although this case does not involve a tailings dam, it falls under the CDA Case 2B, as it lacks both a supernatant pond and liquefiable material.

The potential failure mode was described as: “an undetected weak layer at the saddle berm elevation within the in-pit waste rock dump, coupled with a reduction in waste rock shear strength caused by crushing effects, leads to a translational failure mechanism as the dump is being raised”.

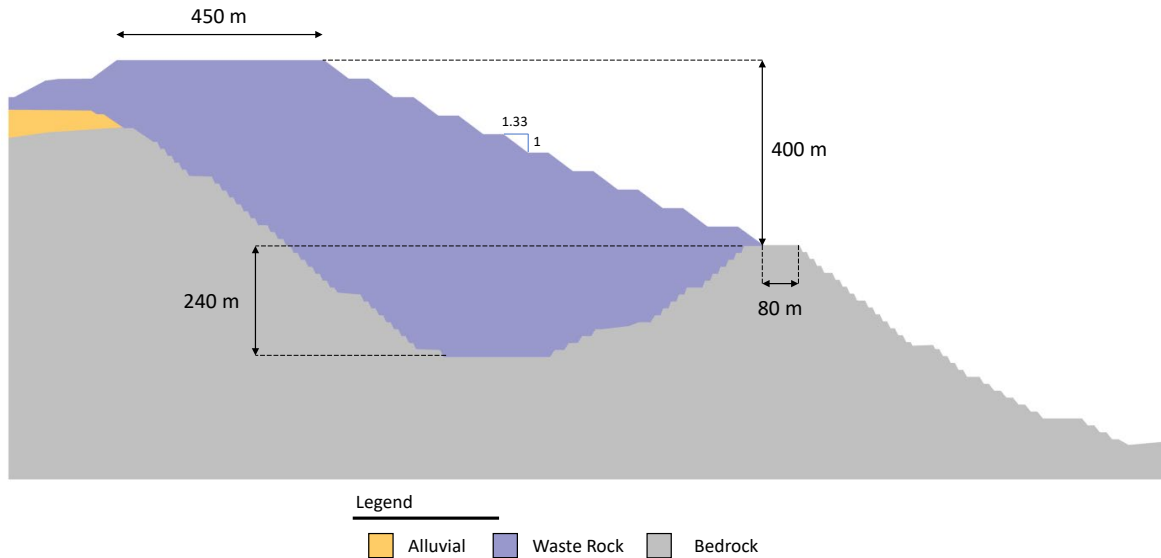


Figure 9: Example 3 – Waste Rock Dump

Figure 10 depicts the MPM model. The analysis included 15,861 material points and 10,387 triangular elements. The weak layer at the saddle berm level represents the failure mechanism. The primary goal was to evaluate the effectiveness of the 80 m wide security berm. The Mohr-Coulomb model was used for all materials, with material properties based on engineering judgment. Table 4 presents the material parameters.

Table 4: Material parameters to achieve equilibrium – Example 3

Parameter	Symbol	Unit	Waste Rock	Alluvial	Weak Layer	Rock
Unit weight	γ	kN/m ³	20.8	18.0	30.8	22.0
Young Modulus	E	MPa	25	15	25	80
Poisson ratio	ν	[-]	0.2	0.2	0.2	0.2
Friction angle	ϕ	°	40	36	40	40
Cohesion	c	kPa	0	0	0	10

The failure was triggered by the combined effects of a weak layer and an abrupt reduction in waste rock shear strength due to crushing. After reaching equilibrium, the weak layer strength was reduced from $\phi = 40^\circ$ and $c = 0$ kPa to $\phi = 0^\circ$ and $c = s_u = 5$ kPa. Simultaneously, the waste rock friction angle was abruptly reduced from 40° to 36° .

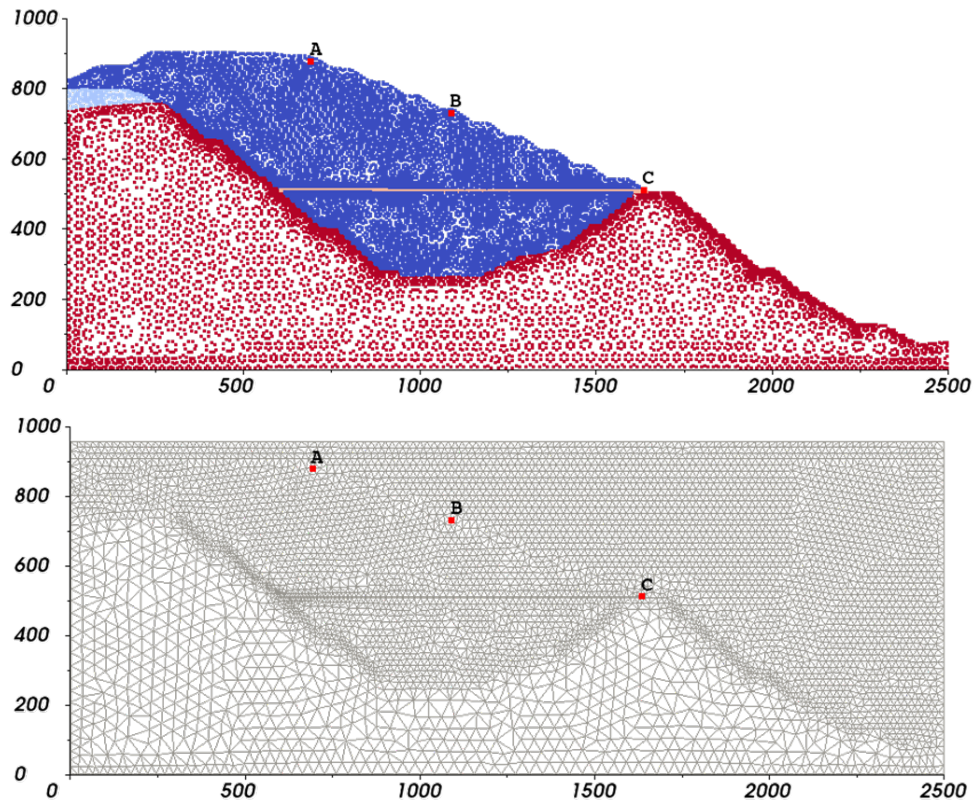


Figure 10: Example 3 – Runout Assessment

Figure 11 shows the results 50 seconds after the movement initiation. The results suggest that, under the assumed failure mode, the berm may not be contain the runout.

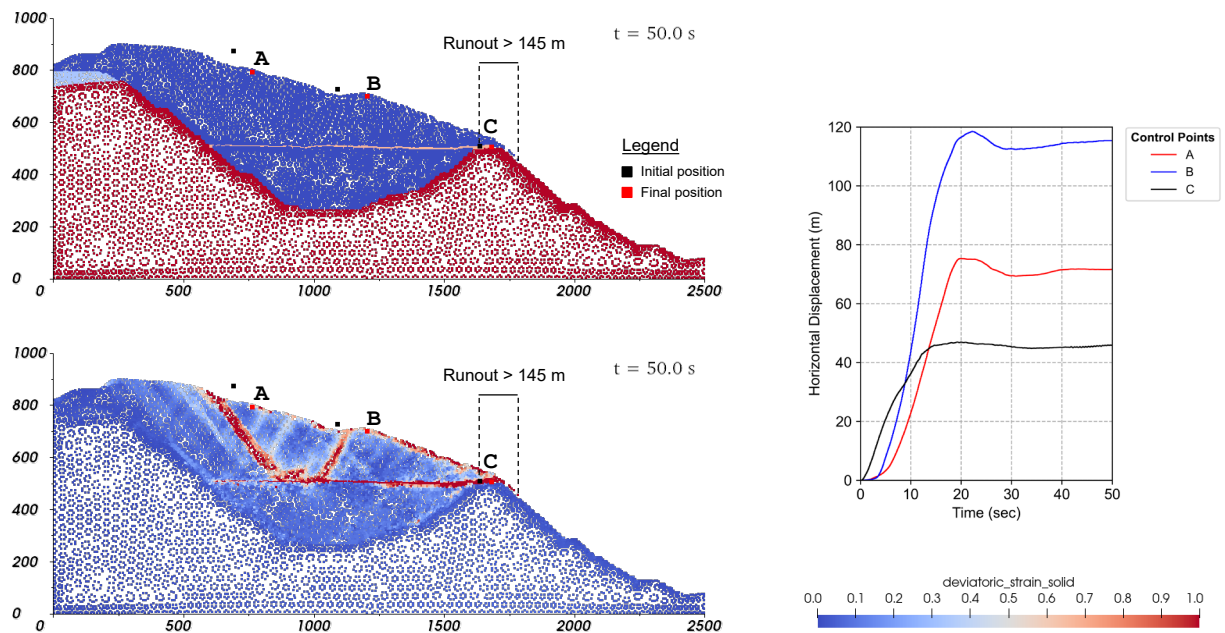


Figure 11: Example 3 – MPM model

5 DISCUSSION OF RESULTS

The MPM simulations for Examples 1, 2, and 3 provide insights into the post-failure behavior of tailings and waste rock under distinct failure modes. The results highlight the role of the failure mechanism, and the shear strength parameters assigned to initiate the movement. Model setup times and runtimes were monitored and found to be acceptable for 2D analyses, with total computational times ranging from a few minutes to under an hour depending on mesh density.

In Example 1, the soft red mud tailings exhibited high mobility following abrupt strength reduction, consistent with thixotropic behavior. A rotational failure released tailings into the environment. Runout distances varied with the remolded shear strength assigned to the low-strength zone (5 kPa and 2 kPa), illustrating the sensitivity of runout predictions to this parameter.

Undrained shear strength values of 5 kPa and 2 kPa, corresponding to the 50th and 20th percentiles of available data, were used to define base and extreme scenarios. The resulting runout distances –31 m for the 50th percentile and 44 m for the 20th percentile– suggest flow-type slope failures without large-scale downstream release.

In Example 2, the filtered tailings dam exhibited a runout of approximately 18 m under the assumed failure mode. Localized saturation of the lower tailings layer was sufficient to initiate displacement. The results indicated that the dam could overtop, releasing filtered tailings into the environment. Despite being compacted during construction, filtered tailings can fail if saturated locally. The observed runout process is consistent with the slumping-type behavior expected for this material under CDA Case 2B.

Example 3 demonstrated that translational failure along a weak layer, combined with a strength loss in waste rock, can result in overtopping into the adjacent open pit. The 80 m security berm was not sufficient to contain the runout, highlighting potential risks to personnel and mining operations. These findings suggest that a larger setback may be required in the design of the in-pit facility. While this may impact the storage capacity of the waste rock dump, a risk-informed design can be developed using the insights gained from the MPM runout assessment.

These results may seem conservative when compared to historical liquefaction cases, but they reflect the assumed failure modes, shear strength parameters and geometric confinement. The discrepancy likely arises from different modeling assumptions: hydromechanical models often represent tailings as highly mobile fluids, leading to overestimated runout distances. In contrast, MPM simulations –such as those presented in this paper– model tailings as saturated soils undergoing abrupt strength loss. This approach does not capture the transition from soil-like to water-like behavior, which is critical for materials with low yield stress and evolving rheology as observed in Adams et al. 2017.

Improved accuracy would require integrating viscous effects and rheological evolution into MPM simulations using models capable of representing phase transitions. These models should capture the transition from frictional and contractive to viscous behavior, which occurs as saturated soil-like tailings evolve into water-like materials during runout. Future work should also benchmark results using tools such as SPH or HEC-RAS –commonly employed for simulating fluid and debris flows– and calibrate against historical failure events. The critical distinction lies not in the tools themselves, but in the constitutive models they employ to realistically capture material response during runout.

6 CONCLUSION

This study demonstrated the use of the Material Point Method (MPM) for runout analysis of CDA Cases 2A and 2B through three application examples. The results highlight MPM's capability to model complex post-failure processes, including flow-type and slumping-type failures, under varying failure modes and shear strength conditions. The example-specific analyses provided valuable insights into tailings and waste rock mobilization, informing risk assessments and key design decisions, such as setback requirements and downstream containment strategies.

MPM proved effective in handling large deformations and modeling low-strength zones without the limitations of conventional numerical methods. However, the analysis has limitations. The simulations do not account for the viscous behavior of tailings, nor do they consider variations in solids content during the runout process. These simplifications may affect the accuracy of the runout estimation for materials undergoing a phase transition from saturated soil-like to water-like behavior, particularly those with low yield stress values observed in rheology tests.

Despite these limitations, MPM shows strong potential as a screening-level tool for tailings dam breach analyses. It provides a high-level view of possible consequences and supports decision-making in early projects stages or for prioritizing risk mitigation. Its application to both CDA Case 2A (flow-type failures driven by contractive behavior) and Case 2B (slumping-type failures in non-liquefiable materials) confirms its versatility for solids-dominated runout assessment.

7 REFERENCES

- Adams, A., Friedman, D., Brouwer, K. and Davidson, S., 2017. Tailings impoundment stabilization to mitigate mudrush risk. In *Proceedings of the 85th Annual Meeting of the International Commission on Large Dams (ICOLD)*
- Al-Kafaji, I.K. Formulation of a dynamic material point method (MPM) for geomechanical problems. PhD Thesis, University of Stuttgart, 2013
- Alonso, E.E., 2021. Triggering and motion of landslides. *Géotechnique*, 71(1), pp.3-59.
- Anura3D MPM Research Community (2024). *Anura3D Version 2024 Source Code*, <www.anura3d.com>
- CDA (Canadian Dam Association). 2021. *Technical Bulletin: Tailings Dam Breach Analysis*.
- Ceccato, F., 2015. Study of Large Deformation Geomechanical Problems with the Material Point Method. Ph.D. thesis. University of Padua, Italy.
- Ceccato, F., Yerro, A., Girardi, V. and Simonini, P., 2021. Two-phase dynamic MPM formulation for unsaturated soil. *Computers and Geotechnics*, 129, p.103876.
- Chen, H and Becker, D. 2014. "Dam Breach Tailings Runout Analysis." Proceedings of Canadian Dam Association, 2014 Annual Conference, Banff, Alberta, Oct. 4–9, 2014.
- Cuomo, S., Ghasemi, P., Martinelli, M. and Calvello, M., 2019. Simulation of liquefaction and retrogressive slope failure in loose coarse-grained material. *International Journal of Geomechanics*, 19(10), p.04019116.
- Di Carluccio, G., Pinyol, N.M., Alonso, E.E. and Hürlimann, M., 2024. Liquefaction-induced flow-like landslides: the case of Valarties (Spain). *Géotechnique*, 74(4), pp.307-324.
- Fern, E.J., Rohe, A., Soga, K., Alonso, E.E., 2019. The Material Point Method for Geotechnical Engineering: A Practical Guide. CRC Press
- International Council on Mining and Metals (ICMM), United Nations Environment Programme (UNEP), Principles for Responsible Investment (PRI), 2020. Global Industry Standard on Tailings Management. <https://globaltailingsreview.org/> Accessed May 22, 2025.
- Leroueil, S., Tavenas, F. and Bihan, J.P.L., 1983. Propriétés caractéristiques des argiles de l'est du Canada. *Canadian Geotechnical Journal*, 20(4), pp.681-705.
- Lino Ramírez, E. 2021. *Modeling of flow liquefaction and large deformations in tailings dams using material point method*. Master Thesis, University of British Columbia.

- Lino Ramírez, E., Taiebat, M. and Lizcano, A., 2023. Flow liquefaction and large deformation analysis in a tailings dam using MPM and critical state-based material modelling. In *10th European Conference on Numerical Methods in Geotechnical Engineering* (pp. 1-6).
- Macedo, J., Yerro, A., Cornejo, R. and Pierce, I., 2024. Cadia TSF failure assessment considering triggering and post triggering mechanisms. *Journal of Geotechnical and Geoenvironmental Engineering*, 150(4), p.04024011.
- Martin, V., Fontaine, D.D., and J.G. Cathcart. 2015. “Practical Tools for Conducting Tailings Dam Breach Studies”. Proceedings of Canadian Dam Association 2015 Annual Conference, Mississauga, ON. Oct. 5–8, 2015.
- Morgenstern N. R., Vick S. G. and Zyl D. V. 2015. “Report on Mount Polley tailings facility breach”. 2015
- Morgenstern N. R., Vick S. G., Viotti C. B. and Watts B. D., “Report on the immediate causes of the failure of the Fundão dam” (commissioned by BHP Billiton Brasil Ltda., Vale S.A., and 20 Samarco Mineração S.A., 2016).
- O’Brien, J.S. 1986. Physical Processes, Rheology, and Modeling of Mud Flows. Ph.D. Dissertation. Colorado State University, Fort Collins, Colorado.
- Robertson P. K., L. de Melo, Williams D. J. and Wilson G. W. Report of the Expert Panel on the Technical Causes of the Failure of Feijão dam I. 2019
- Small, A., James, M. and M. Al-Mamun. 2017. “Advancing the State of Practice for Tailings Assessment Using Empirical Correlations”. Proceedings of the Canadian Dam Association 2017 Annual Conference, Kelowna, BC, Oct. 16–18, 2017.
- Sulsky, D., Chen, Z. and Schreyer, H.L., 1994. A particle method for history-dependent materials. *Computer methods in applied mechanics and engineering*, 118(1-2), pp.179-196.
- Sulsky, D., Zhou, S.J. and Schreyer, H.L., 1995. Application of a particle-in-cell method to solid mechanics. *Computer physics communications*, 87(1-2), pp.236-252.
- U.S. Bureau of Reclamation, 1988, *Downstream Hazard Classification Guidelines*, ACER Technical Memorandum No. 11, Assistant Commissioner-Engineering and Research, Denver, Colorado, December 1988, 57 p.
- Wei, Z., Yin, G., Wang, J.G., Wan, L. and Li, G., 2013. “Design, construction and management of tailings storage facilities for surface disposal in China: case studies of failures”. *Waste Management & Research*, 31(1), pp.106-112.
- Williams H., Hockley D., LePoudre C. and Kozikowski M. 2023. “Limitations and Possible Improvement of Dam Breach Studies”. Proceedings of Tailings and Mine Waste 2023. Vancouver, Canada. November 5-8, 2023.
- Yerro, A., 2015. MPM Modelling of Landslides in Brittle and Unsaturated Soils. Ph.D thesis. Univesitat Politècnica de Catalunya, Spain.
- Yerro, A., Alonso, E.E. and Pinyol, N.M., 2016. Run-out of landslides in brittle soils. *Computers and Geotechnics*, 80, pp.427-439.
- Yerro, A., Soga, K. and Bray, J., 2019. Runout evaluation of Oso landslide with the material point method. *Canadian Geotechnical Journal*, 56(9), pp.1304-1317.
- Yerro, A., Girardi, V., Martinelli, M. and Ceccato, F., 2022. Modelling unsaturated soils with the Material Point Method. A discussion of the state-of-the-art. *Geomechanics for Energy and the Environment*, 32, p.100343.